Applied Surface Science 620 (2023) 156777

Contents lists available at ScienceDirect

Applied Surface Science

journal homepage: www.elsevier.com/locate/apsusc

Full Length Article

Molecular properties of PTCDA on graphene grown on a rectangular symmetry substrate

Haojie Guo [a,*], Antonio J. Martínez-Galera [b,c,*], José M. Gómez-Rodríguez [a,c,d,1]

[a] Departamento de Física de la Materia Condensada, Universidad Autónoma de Madrid, E-28049 Madrid, Spain
[b] Departamento de Física de Materiales, Universidad Autónoma de Madrid, E-28049 Madrid, Spain
[c] Instituto Nicolás Cabrera, Universidad Autónoma de Madrid, E-28049 Madrid, Spain
[d] Condensed Matter Physics Center (IFIMAC), Universidad Autónoma de Madrid, E-28049 Madrid, Spain

ARTICLE INFO

Keywords:
PTCDA molecule
2D materials
Symmetry mismatched substrates
Quasi-1D moiré patterns
Self-assembled growth
Molecular orbitals

ABSTRACT

The chemical modulation associated with moiré patterns, arising at the interface of metal-supported 2D material systems, affects the interaction between molecules and 2D materials on surfaces. Since the crystallography of the support influences the interfacial chemistry of the moiré modulation, this parameter could also play a role in the graphene-molecule interaction, although studies using non-hexagonal metal supports are needed to investigate this effect. It is a key issue since graphene appears combined with organic films in most technological advances related to this material. Here, we have characterized the properties of PTCDA molecules on graphene grown on Rh(110) substrates, which exhibit a rectangular atomic packing, using scanning tunneling microscopy and spectroscopy. The results showed that PTCDA molecules are arranged on the surface into a herringbone structure exhibiting a long-range ordering, which grows continuously across substrate atomic steps edge and dislocations. The quasi-1D moiré patterns of the Gr/Rh(110) surfaces are found to provide an inert chemical landscape for the molecular arrangement. Bias voltage-dependent imaging of the orbital structure of PTCDA molecules and differential conductance spectra back up a weak molecule–substrate interaction scheme. Finally, the α-polymorph of bulk crystal PTCDA has been determined as the favored stacking configuration for bilayer molecules on Gr/Rh(110).

1. Introduction

The rise of two-dimensional (2D) materials has enabled their extensive use, in recent years, as a platform for molecular adsorption studies [1–4], aimed to tune their properties [5], understand the intrinsic properties of molecular adsorbates on these surfaces [2,6], and grasp the interfacial properties for potential implementation in the forthcoming technologies [3,7]. This is due, on the one hand, to the generally low reactivity of most of the 2D materials, which makes them very useful for the electronic decoupling of molecular adsorbates from the substrate, allowing a detailed study of their properties [2]. On the other hand, the properties of interfaces composed of a 2D material and a substrate can be selected, within a wide range, by appropriately combining both components [8–11]. This opens the door to modifying, in a controlled manner, their interaction with adsorbates, and consequently the growth of molecular structures, by appropriate choice of the 2D material/substrate interface. This issue has important implications facing the development of technological applications given the fact that in the most transcendental advances related to 2D materials, they are combined with organic compounds, which has allowed, for instance, the development of flexible touchscreens [12,13], organic field-effect transistor [14], or organic solar cells [15].

Some 2D materials as graphene and hexagonal boron nitride (h-BN) grown on metal surfaces are characterized by the formation of long-range spatial and chemical modulations known as moiré patterns [8,9]. These repeating structures, whose main features strongly depend on the underlying metal geometry [10], have been demonstrated to provide a complex chemical landscape for the adsorption of molecules. The chemical modulations associated with moiré patterns are responsible for a varied phenomenology, ranging from merely physisorption interaction to form closely packed molecular assemblies [6,7,16], to site-specific chemical bonding of the molecules within preferential

* Corresponding authors.
E-mail addresses: haojie.guo@uam.es (H. Guo), antonio.galera@uam.es (A.J. Martínez-Galera).
[1] Deceased.

https://doi.org/10.1016/j.apsusc.2023.156777
Received 18 December 2022; Received in revised form 31 January 2023; Accepted 14 February 2023
Available online 19 February 2023

positions of the moiré supercell [17,18]. All these effects are conditioned by the specific interfacial chemistry landscape, which is governed by the symmetry, periodicity and corrugation of the moiré patterns [10]. These effects have been extensively investigated for graphene and h-BN monolayers grown on metal surfaces with hexagonal atomic packing. As a result, it has been demonstrated that effects such as site-specific chemical bonding of the molecules within preferential positions of the moiré supercells [18–20], templated growth of molecular structures [21–24], or molecular adsorption involving significant charge transfer [18,25] occurs when the interfacial bonding landscape is ruled by the existence of two chemical environments for the atoms of the 2D material [2,9]. However, studies of these effects on 2D materials resting on metal supports with rectangular or square symmetries are scarce. Therefore, a complete picture of the wide range of possibilities offered by metal-supported 2D materials for molecular adsorption and thin film growth is still lacking. This issue is of paramount significance given the fact that among the most widespread supports for graphene growth are polycrystalline thin films, which are composed of grains exhibiting different crystallography, and hence showing distinct atomic packing geometries [11,26,27].

Graphene monolayers grown on metal supports with square or rectangular symmetries give rise to the formation of quasi-1D moiré patterns [28–31]. Among them, the surfaces of the Gr/Rh(110) interface present interesting properties to, either demonstrate or discard, a correlation between the interfacial chemistry and effects associated with the molecule–substrate interaction as moiré templated growth of molecular structures, molecule-graphene charge transfer or the selective bonding of the molecular adsorbates, in certain regions of the 1D moiré superstructures formed on non-hexagonal symmetric supports [31]. In particular, a recent XPS study suggests that, on the surface of Gr/Rh (110), there are two distinctive chemical bonding-state of C atoms, related to the existence of different chemical landscapes associated with the quasi-1D moiré patterns formed at the interface of Gr/Rh(110). Therefore, in light of the generally accepted view in the literature, the presence of this chemically modulated quasi-1D moiré patterns of Gr/Rh (110) substrate should potentially affect the adsorption of molecules. On the other hand, ARPES data on Gr/Rh(110) indicate the conservation of Dirac cones in this system, so that graphene preserves its most representative properties [31].

The π-conjugated semiconducting molecule 3,4,9,10-Perylenetetracarboxylic dianhydride (PTCDA) has stood up as a prototype molecule for fundamental studies to understand the behavior of molecular adsorbates on solid surfaces, and also for its suitability in applications based on optoelectronic devices [32]. In this sense, PTCDA molecules have been characterized before using different experimental techniques on low-index surfaces of noble metals [33–47], on semiconductors [48–50] like silicon or germanium, on graphite [34,51–55] and, lately, on 2D materials [6,7,22,23,34,53,55–61]. Different arrangements of PTCDA on these surfaces have been documented, which are correlated with the form in which the molecule interacts with the underlying substrate, from weak physisorptive to stronger chemisorptive interaction.

In this work, the effects of chemically modulated quasi-1D moiré patterns, arising from graphene grown on Rh(110) [31], on the adsorption and electronic properties of PTCDA molecules have been investigated *via* scanning tunneling microscopy and spectroscopy (STM/STS) under ultra-high vacuum (UHV) conditions at room temperature (RT). The results shed light on a weak molecule–substrate interaction regimen, where the molecules form the well-known herringbone structure, stabilized by intermolecular forces. The molecular ordering of PTCDA is unperturbed by the quasi-1D moiré patterns of Gr/Rh(110), and our spectroscopic results demonstrate the absence of a significant molecule-graphene charge transfer. These findings differ from the available literature on hexagonally symmetric moiré patterns, where the existence of distinctive chemical regions within the moiré unit cell of 2D material/metal systems was found to affect molecular adsorption.

2. Experimental methods

All sample preparation and characterization were carried out in two interconnected UHV chambers (base pressure below 10^{-10} Torr) equipped, respectively, with standard surface preparation facilities and a custom-built Variable Temperature Scanning Tunneling Microscope (VT-STM) [62]. Single crystal Rh(110) surfaces were prepared through sputtering with Ar^+ at 1 keV, followed by annealing at 950 °C in an oxygen atmosphere ($P_{oxygen} = 2 \times 10^{-6}$ Torr), and finishing with a flash annealing at 1050 °C. Graphene monolayers were then grown on Rh (110) by high-temperature decomposition of ethylene (C_2H_4). Specifically, the Rh(110) surfaces were kept at 900 °C and exposed to 45 L of ethylene at a partial pressure of 3×10^{-7} Torr. The quality of the as-grown samples was checked by STM before any molecule deposition. PTCDA molecules were sublimated from a home-built tantalum crucible, thoroughly outgassed beforehand, at a deposition rate ≈ 0.2 ML/min, while maintaining the Gr/Rh(110) substrate at RT. The deposition rate was calibrated by STM imaging.

STM images were acquired in the constant current mode and with bias voltage applied to the sample, while the tip, made of tungsten, remains grounded. All STM/STS measurements were performed at RT. The data acquisition, analysis and rendering were accomplished by using the WSxM software [63].

3. Results and discussion

To facilitate the understanding of the properties of PTCDA molecules on Gr/Rh(110), it is noteworthy to give a brief description of the main structural properties of this substrate. Fig. 1 shows representative STM images acquired on Gr/Rh(110) surfaces before the deposition of PTCDA molecules on them. As can be observed, the surface of graphene grown on Rh(110) is characterized by the appearance of different moiré patterns, featuring, in the present case, a quasi-1D geometry. This particular quasi-1D moiré pattern geometry arises from the symmetry mismatch between graphene (sixfold) and the underlying Rh(110) (twofold). Despite the existence of different possible moiré patterns on this substrate, caused by the multiple rotational domains of graphene on Rh (110), they can be classified into two types. The first type corresponds to moiré patterns featuring a single set quasi-1D fringe over the surface, with a periodicity of ≈ 1 nm (see Fig. 1a–b). This corresponds mainly to rotational domains, where graphene is aligned, or closed to be aligned, with the [001] direction of Rh(110). Meanwhile, in the second type, the moiré patterns are composed of two sets of quasi-1D fringes: one with a periodicity of ≈ 1 nm, and another with a periodicity of ≈ 2–6 nm (which depends on the exact misorientation between graphene and Rh (110)). Examples of this last type of moiré pattern can be observed in Fig. 1c–d. Further details on the structural and electronic properties of the Gr/Rh(110) surface can be found in the reference [31].

A general view of the sample morphology after depositing a submonolayer coverage of PTCDA molecules on Gr/Rh(110) can be observed in Fig. 2a. The molecules form a well-ordered, compact, widely extended molecular assembly with a low defect concentration, indicating a high crystalline quality of the PTCDA adlayer. By taking a closer look into this molecular arrangement, a herringbone structure, consisting of two molecules per unit cell, is observed in STM images as that shown in Fig. 2b. The experimental values of the moduli of the herringbone unit cell vectors, $\vec{b_1}$ and $\vec{b_2}$, have been determined to be 2.0 ± 0.2 nm and 1.3 ± 0.2 nm, respectively, whereas the relative angle, θ, between both vectors has been found to be 95° ± 5°. To aid in the visualization, a schematic representation of the herringbone structure, outlining the molecule orientation within the unit cell, is depicted in Fig. 2c.

This herringbone structure of PTCDA, with similar lattice constants, has been reported before on substrates that give rise to a weak molecule–substrate interaction, such as Au(111) [33,35,42,47], graphite

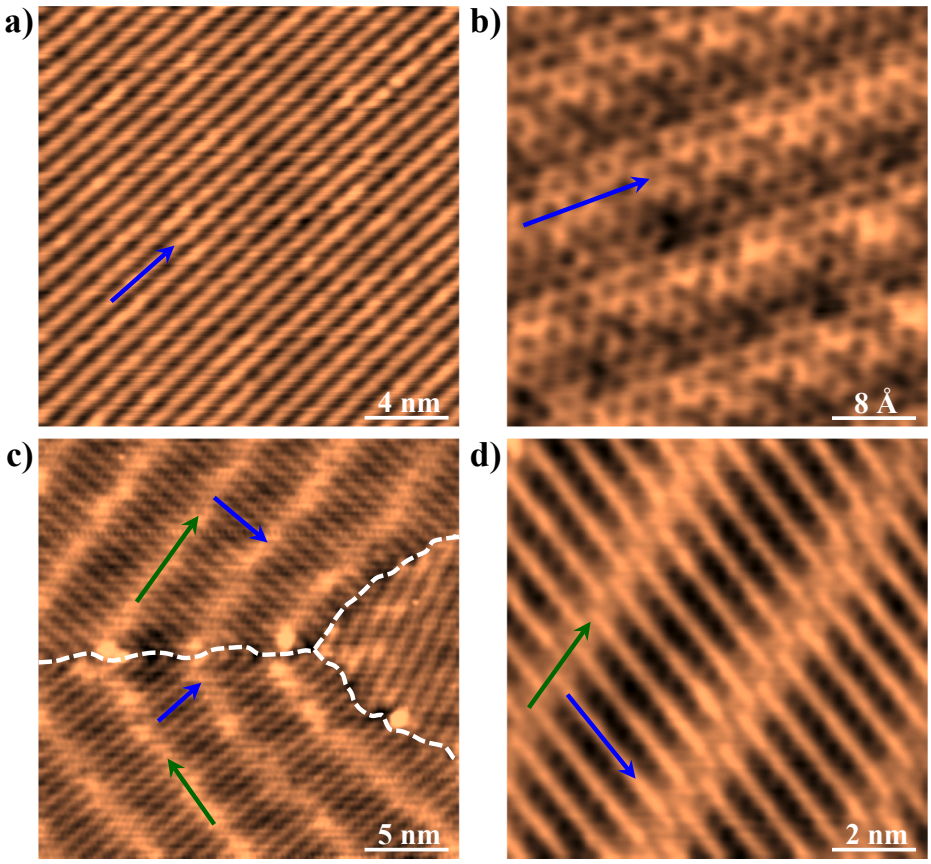

Fig. 1. Quasi-1D moiré patterns observed on Gr/Rh (110) surfaces. a) STM image of a sample region where a single set of quasi-1D moiré fringes (marked by the blue arrow) can be observed. b) Atomically resolved STM images acquired on a region with a single moiré pattern. c) STM image showing the boundaries (highlighted by the dashed white line) between different rotational domains of graphene. In each domain, the Gr/Rh(110) surface features quasi-1D moiré patterns with different orientations. In these cases, the moiré patterns are composed by two sets of quasi-1D fringes (indicated by the blue and green arrows). d) Zoom-in STM image showing this type of moiré patterns. Tunneling parameters: a) $V_s = 2$ V; $I_t = 0.3$ nA; 20×20 nm^2. b) $V_s = 0.46$ V; $I_t = 15$ nA; 4×4 nm^2. c) $V_s = 1$ V; $I_t = 0.5$ nA; 25×25 nm^2. d) $V_s = 1.4$ V; $I_t = 6.5$ nA; 10×10 nm^2.

[34,51–55], graphene [6,7,22,23,57–60,64], TMDs [34,53,55,56], and h-BN [24,61]. Likewise, it also closely resembles that found on a few layers PTCDA [38,41,65] and in the (102) plane of the bulk crystal [66–68]. However, when adsorbed on surfaces giving rise to strongly interacting (chemisorption) molecule–substrate systems like the low-index ones of Ag [44,45,69], Cu [39,46] and semiconductors [48–50], PTCDA molecules adopt a wide range of structures, from the brick wall assembly to disordering. Some previous investigations on this molecule have indicated that the herringbone structure is stabilized through the quadrupolar and hydrogen bonding interaction between neighbor molecules [43,53]. Hence, it is reasonable to suggest that the molecular assembly of PTCDA on Gr/Rh(110) is dominated mainly by intermolecular forces rather than by molecule–substrate interaction, which, in turn, could imply that the latter should be weak compared with the former. This predominant role of the cohesive intermolecular forces is further reinforced by the fact that single isolated PTCDA units on the surface were not observed at RT.

The arrangement of PTCDA across extended defects in the supporting surface and molecular domain boundaries has also been explored. Fig. 3a shows a typical STM image acquired around the edge of a single atomic step of Rh(110), as deduced from the apparent height profile, where the PTCDA monolayer grows uniformly along with it. Similarly, the molecular arrangement of PTCDA flows continuously throughout substrate dislocations (green circle), as observed in STM images as that shown in Fig. 3b. Oppositely, the PTCDA overlayer is perturbed in the frontier between two graphene rotational domains (Fig. 3c) and adopts different orientation registries. The presence of different graphene domains is inferred based on the observation of the long-range fringes-like patterns in the image superimposed over the molecular layer, which are not oriented in the same direction on both sides of the boundary. This is related, probably, to the existence of different quasi-1D moiré patterns of Gr/Rh(110), originating from different orientations of graphene over the metal [31], at both sides of the molecular layer. Likewise, as observed in Fig. 3d, the translational domain boundary between two molecular wavefronts also impacts the continued growth of the molecular adsorbates.

The continuous flow of PTCDA molecules along edge steps and dislocations can be understood in terms of the uniformity, flatness and high quality of graphene underneath, which also grows continuously across these extended defects of the Rh(110) surface. Therefore, graphene monolayers reduce the interaction of the molecular adlayer with these substrate defects, allowing it to grow homogeneously. Comparable assembly properties of PTCDA on other 2D material systems have been addressed before [7,24,57,61]. In contrast, frontiers of rotational domain boundaries of graphene, defined as grain boundaries, proceed as a barrier to the uninterrupted expansion of PTCDA molecules over the surface. This could be explained as the result of an enhanced molecule-graphene interaction at those locations, due to the fact that the crystalline symmetry of graphene is broken, and the graphene sheet is no longer continuous over these areas. Therefore, the molecular layer may adopt different orientations at both sides of the grain boundaries. Also, the molecular arrangement is disrupted across translational molecular boundaries, which are caused by the unbiased initial nucleation position of PTCDA on graphene, due to the chemical inertness of the latter [70], which triggers a lateral shift of the molecular assemblies.

To shed light on the possible influence of the underlying substrate on the self-assembly of PTCDA molecules, a detailed analysis of the molecular cell orientation with respect to the underlying quasi-1D moiré pattern has been performed. Fig. 4a–f show a set of STM images acquired at the edge between molecular islands and an uncovered region of the substrate, where the PTCDA arrangement and the substrate quasi-1D moiré pattern are simultaneously imaged. Different twist angles, ranging from 43° to 90°, as indicated in each image, between the shorter unit cell vector, $\vec{b_2}$, of the herringbone structure of PTCDA and the moiré

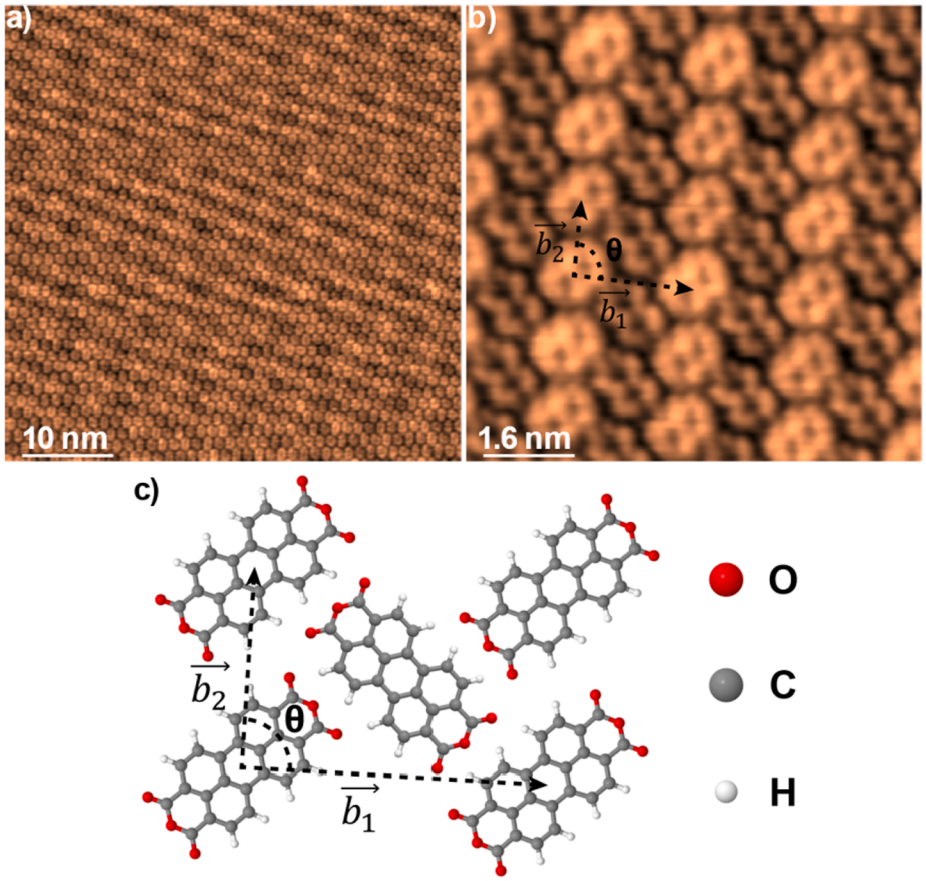

Fig. 2. Herringbone structure of PTCDA molecules on Gr/Rh(110). a) General overview of the molecular arrangement of PTCDA adsorbed on Gr/Rh (110). b) A magnified STM image on a molecular island showing that PTCDA molecules form a herringbone structure. The unit cell vectors and their relative angle are represented by $\vec{b_1}$, $\vec{b_2}$ and θ, respectively. c) Schematic drawing of the herringbone structure of PTCDA. Tunneling Parameters: a) $V_s = -2.1$ V; $I_t = 0.57$ nA; 50×50 nm^2. b) $V_s = 1.2$ V; $I_t = 0.9$ nA; 8×8 nm^2.

fringes direction have been observed. Moreover, a faint long-range modulation, which is present in the Gr/Rh(110) substrate, can also be noticed in some molecular assemblies like those in Fig. 4b,e.

Given the results presented in Fig. 4, it is clear that the quasi-1D moiré patterns of Gr/Rh(110) do not have a major effect on the ordering of PTCDA molecules, which is in agreement with the weak molecule–substrate interaction argued above. However, this result is in contrast with the available literature on hexagonal symmetric moiré patterns. Generally, the presence of different chemical landscapes induced by the moiré patterns on the surfaces of 2D material/metal substrates modifies the adsorption behavior of molecules [2,11]. For example, some subregions within the moiré patterns of Gr/Ru(0001) or h-BN/Rh(111) can act as trapping areas for C_{60} and CuPc molecules, respectively [18,19]. Additionally, the chemically modulated moiré patterns can act as a template for the growth of different nanostructures of molecules [21,24]. In the present case, none of these effects is observed for PTCDA on Gr/Rh(110), despite that the graphene layer also shows marked variations in the chemical landscape associated with the presence of quasi-1D moiré patterns, as demonstrated previously by XPS measurements [31]. Therefore, the results obtained here constitute a singular addition to the generally accepted view of the adsorption of molecules on metal-supported 2D material substrates.

On the other hand, the weak long-range modulation observed in Fig. 4b,e and also in Fig. 3b–c could be explained on the basis of one of the two sets of stripes, characteristic of the complex moiré patterns resulting in certain rotational angles of graphene sheet on Rh(110), as described previously [31] (see also Fig. 1). Similar visualization of substrate structural features through the molecular layer has been observed for PTCDA on Au(1 1 1) [42], where the $22 \times \sqrt{3}$ surface reconstruction appears superimposed to the molecular assembly, and also on Gr/Ru(0 0 0 1) [22,23] and h-BN/Rh(111) [24] where the highly corrugated moiré patterns can be imaged through the molecular layer. Contrary, this is not the case for PTCDA on Gr/Pt(111) [6], h-BN/Pt (111) [24] or h-BN/Rh(110) [61]. Another dazzling feature observed in those images shown in Fig. 4 is the noisy border of the molecular islands, which could be due to a combination of thermal and tip-induced motion of PTCDA molecules.

To further elucidate the level of interaction between molecule and substrate, the frontier molecular orbital geometries of PTCDA on Gr/Rh (110) have been imaged at RT, and complemented with differential conductance spectra. Fig. 5a shows a STM image acquired at a sample voltage of −2 V, showing an eight lobes intramolecular feature. A zoom-in image of an individual molecule is depicted in the bottom left. For comparison, the DFT calculated theoretical Highest Occupied Molecular Orbital (HOMO) structure of the free molecule [42] is shown in the top left. Fig. 5b illustrates a STM image acquired at a bias voltage of +1.1 V, where molecules exhibit a ten lobes submolecular feature. Similarly, the theoretically calculated Lowest Unoccupied Molecular Orbital (LUMO) structure of the free molecule [42] and a magnified STM image on a single molecule are depicted on the left. Moreover, a numerical differentiated I-V plot (being the average of five individual I-V traces), which reflects the LDOS of the sample, measured on top of a PTCDA molecule on Gr/Rh(110), is shown in Fig. 5c. Two pronounced peaks, centered at a sample voltage of ≈ -2.0 V and $\approx +1.0$ V, can be discriminated in the graphics.

The high similarity between the experimentally measured intramolecular features and the theoretical ones, corresponding to the HOMO and LUMO structures of the free-standing molecule [42], suggests that those submolecular protrusions resolved in Fig. 5a–b could be related, respectively, with the HOMO and LUMO structures of PTCDA on Gr/Rh (110). This may also imply a weak molecule–substrate interaction since the molecular orbitals are not perturbed compared with the free molecule, which is at variance, for instance, with the case of PTCDA on Si (111)-(7 × 7), characterized by a strong molecule–substrate interaction

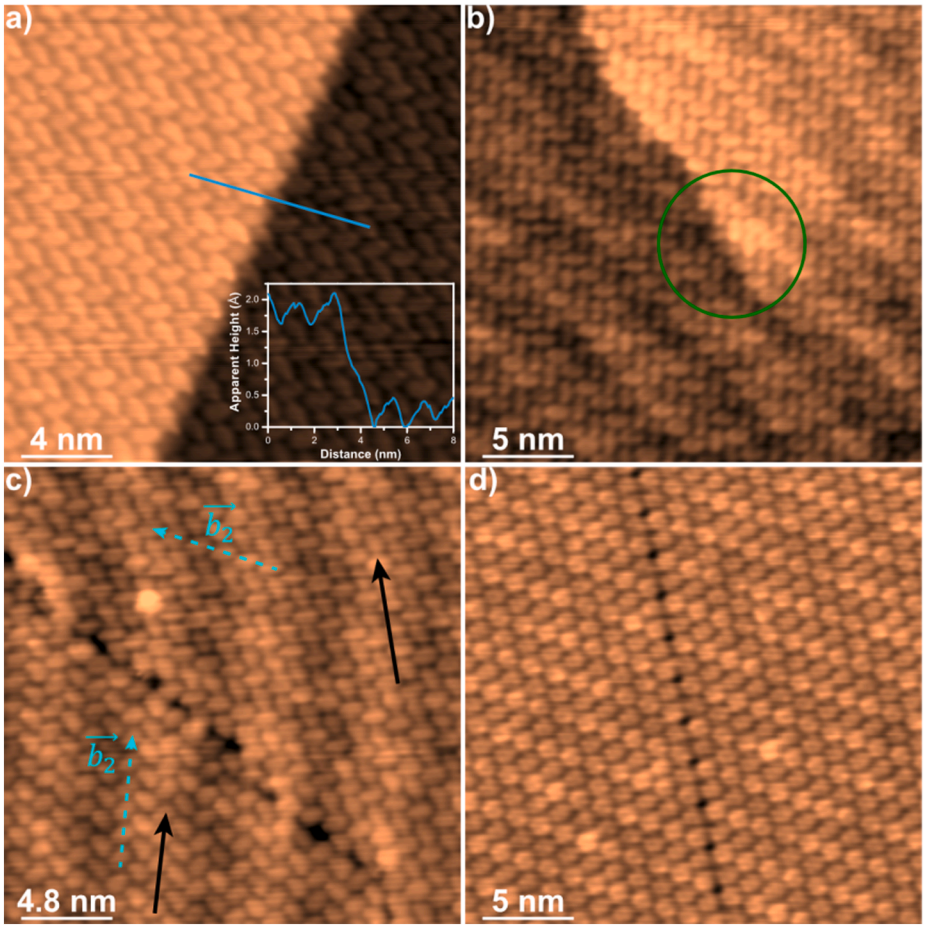

Fig. 3. Behavior of PTCDA molecules across extended defects of Gr/Rh(110) and molecular domains. a,b) Smooth growth of monolayer PTCDA across single atomic step and dislocation of the substrate Rh(110) beneath graphene. c,d) Corresponding STM images showing that the molecular layers are truncated near rotational and translational domains boundary. The black arrows in (c) indicate the direction of the quasi-1D moiré patterns of the Gr/Rh(110) substrate at both side of the molecular domains. Tunneling parameters: a) $V_s = -2.1$ V; $I_t = 0.1$ nA; 20×20 nm^2. b) $V_s = -2.1$ V; $I_t = 0.13$ nA; 25×25 nm^2. c) $V_s = -2.1$ V; $I_t = 90$ pA; 25×25 nm^2. d) $V_s = -2.1$ V; $I_t = 0.1$ nA; 25×25 nm^2.

[48]. Besides, akin molecular orbitals structures have also been reported for PTCDA physisorbed on Au(111) [42], Gr/Pt(111) [6], Gr/Ru(0001) [22] and h-BN/Rh(110) [61], where a weak molecule–substrate interaction is attributed in all these cases. Taking into account the bias voltage at which the molecular orbitals were observed in STM images as those displayed in Fig. 5a–b, the two major peaks in Fig. 5c can be ascribed to the HOMO and LUMO resonances of PTCDA on Gr/Rh(110). Their energy positions are comparable, within the uncertainty associated with RT measurements, to previous STS studies of PTCDA on gold substrates [37,40,42,55], graphene [6,7], graphite [55], and h-BN [61]. Thus, the interaction between PTCDA and Gr/Rh(110) can be regarded as weak, where chemisorptive interaction should not take place, and where charge transfer, if any, should be negligible. Again, this result differs from other 2D material/metal systems where the moiré patterns show a distinctive chemical bonding scheme [2,11]. In these substrates, the pristine electronic properties of the molecules are generally perturbed. This is, for instance, the case of C_{60} molecules on Gr/Ru(0001), where the interaction with the substrate induces a change in the energy level alignment of the LUMO state of the molecule [18]. It, in turn, could imply changes in the properties of graphene, which should be taken into account facing future technological applications, involving the combination of this 2D material and organic thin films.

As a final issue, the stacking configuration of bilayer PTCDA has been investigated. It is known that there are two polymorphs of bulk crystal PTCDA, namely α and β, whose main difference resides in the vertical stacking configuration of the (102) molecular plane [36,66,68] (see Fig. 6a). Both consist of a translation of the unit cell in the consecutive layers along either the lattice vector $\vec{b_1}$ (α) or $\vec{b_2}$ (β). Fig. 6b shows a typical STM image of the bilayer and monolayer PTCDA molecular terraces. The second and first layer's herringbone unit cells are highlighted by the dashed green and solid black rectangle, respectively. An extension of the short $\vec{b_2}$ vector is represented by the dotted black line. The apparent height of the second layer has a value of ≈ 3 Å, as can be deduced from the lateral cross-section depicted in Fig. 6c.

As can be observed from Fig. 6b, the unit cell of the second layer appears shifted along the $\vec{b_1}$ direction by ≈ 4–5 Å, which would correspond to α polymorph. This stacking behavior is identical for bilayer PTCDA on h-BN/Rh(110) [61] and for multilayers PTCDA on Ag(110) [41] or Ag/Si(111) [65]. The existence of possible changes in the lateral dimensions of the molecular unit cell of the second layer, as referred to their counterparts of the first one, has not been appreciated within the experimental error of STM imaging. Moreover, the height of the bilayer PTCDA is consistent with the distance between consecutive layers of PTCDA in the (102) plane of the bulk crystal [66].

4. Conclusions

In summary, we have investigated the effect of the chemically modulated quasi-1D moiré patterns of Gr/Rh(110) on the structural and electronic properties of PTCDA molecules by means of STM and STS at RT. Our experimental results demonstrate that the PTCDA molecules self-assemble forming a well-ordered herringbone structure, where the underlying substrate defects, like atomic steps or dislocations, do not disturb its continuous growth over the surface. Only domain boundaries between two graphene flakes or different molecular wavefronts can alter its crystalline growth on the substrate. A significant impact of the chemically modulated quasi-1D moiré patterns of Gr/Rh(110) on the molecular ordering of PTCDA has not been observed, suggesting a weak molecule–substrate interaction. This weak-molecule substrate

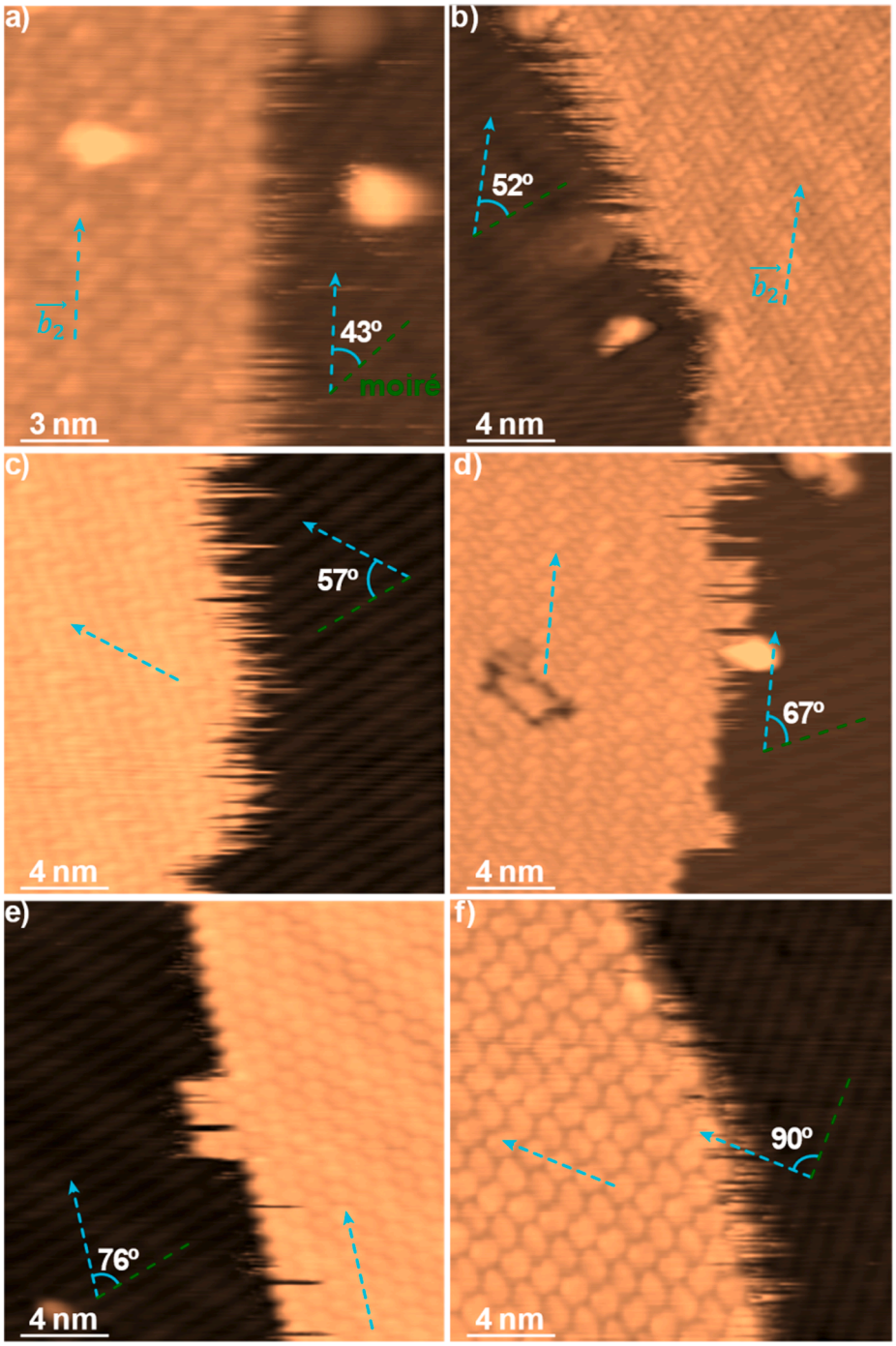

Fig. 4. Influence of the Gr/Rh(110) substrate on the molecular assembly of PTCDA. a–f) Selection of STM images acquired at the edge of a molecular island of PTCDA, and where the bare Gr/Rh(1 1 0) region is also observed at the same time. In all the images, the quasi-1D moiré pattern of Gr/Rh(110) is indicated by the green dotted line whereas the short direction, $\vec{b}_2$, of the herringbone unit cell is highlighted by the cyan dashed arrow. As can be deduced from the different angles between the moiré fringes and the $\vec{b}_2$ direction, the PTCDA ordering seem not to be affected by the moiré stripes. Tunneling parameters: a) $V_s = -2.0$ V; $I_t = 20$ pA; 15×15 nm^2. b) $V_s = 2.0$ V; $I_t = 20$ pA; 20×20 nm^2. c) $V_s = 2.1$ V; $I_t = 20$ pA; 20×20 nm^2. d) $V_s = 2.0$ V; $I_t = 30$ pA; 20×20 nm^2. e) $V_s = -2.1$ V; $I_t = 20$ pA; 20×20 nm^2. f) $V_s = -2.1$ V; $I_t = 35$ pA; 20×20 nm^2.

interaction is further supported through the similarity of the HOMO and LUMO structures of PTCDA on Gr/Rh(110) with the theoretically calculated ones for the free-standing molecule. Point spectroscopy data also endorse a weak interaction between molecule and substrate, with negligible charge transfer. These results are at variance with other 2D material/metal systems, where the presence of distinctive chemical regions within the moiré patterns unit cell affects drastically the adsorption properties of the molecules. Finally, bilayers of PTCDA adopt the α-stacking configuration with respect to the first layer. This work constitutes an experimental demonstration that the existence of a marked chemical modulation on the moiré patterns does not necessarily affect the adsorption of molecules. This information is important in facing the future development of technological applications combining graphene and organic thin films.

CRediT authorship contribution statement

Haojie Guo: Data curation, Formal analysis, Investigation, Validation, Visualization, Writing – original draft, Writing – review & editing. **Antonio J. Martínez-Galera:** Conceptualization, Funding acquisition, Project administration, Supervision, Methodology, Validation, Writing – review & editing. **José M. Gómez-Rodríguez:** Funding acquisition, Resources, Software, Supervision.

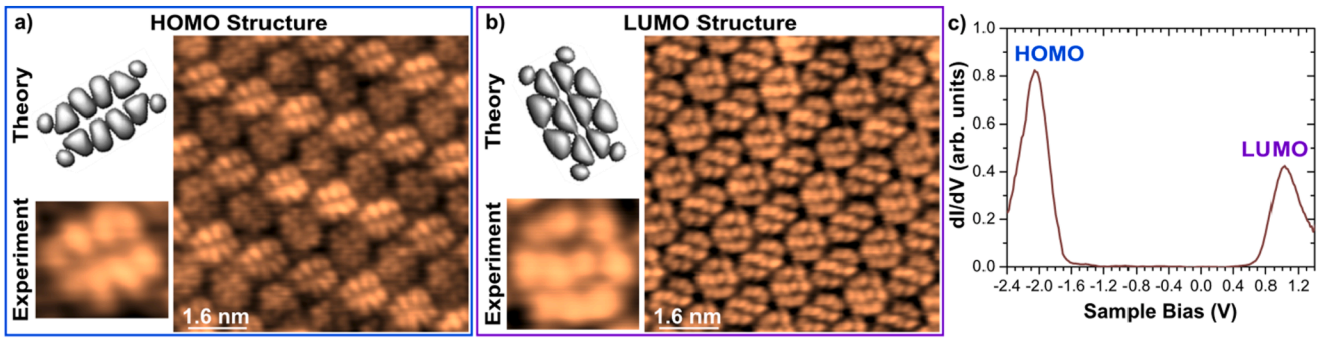

Fig. 5. Electronic properties of monolayer PTCDA on Gr/Rh(110) at RT. STM images of the HOMO (a) and LUMO (b) intramolecular features of PTCDA adsorbed on Gr/Rh(110). Theoretical calculated HOMO and LUMO structure of the free molecule, adapted from [42], as well as a magnified image on a single molecule are depicted in the left of each panel. c) dI/dV curve obtained by numerical differentiation from the average of five I–V curves measured on a PTCDA molecule. Two major peaks can be observed, which are ascribed to the HOMO and LUMO resonances. Tunneling parameters: a) $V_s = -2.0$ V; $I_t = 0.8$ nA; 8×8 nm^2. b) $V_s = 1.1$ V; $I_t = 0.8$ nA; 8×8 nm^2. Stabilization parameters: c) $V_s = 2.0$ V; $I_t = 0.6$ nA.

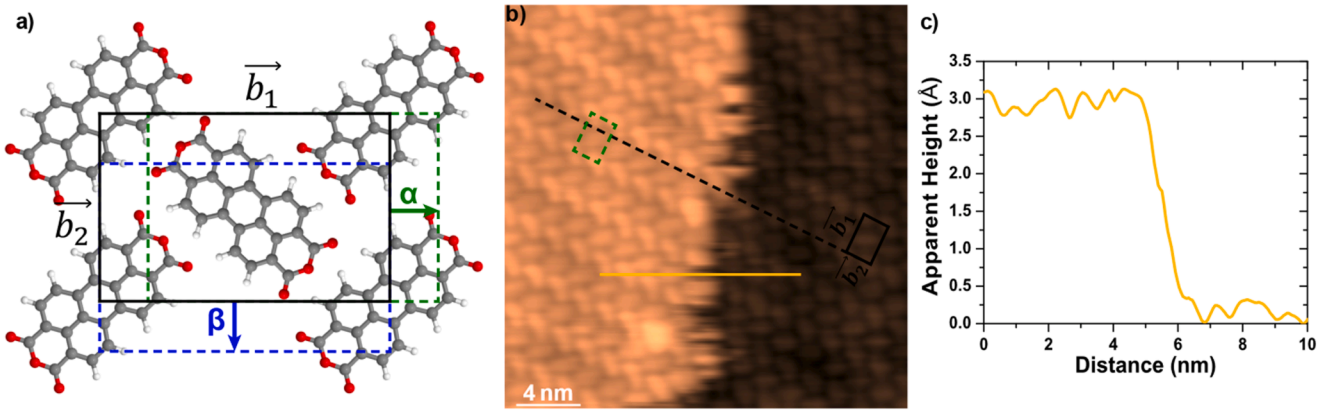

Fig. 6. Polymorphism of bilayer PTCDA on Gr/Rh(110). a) Schematic representation of the α and β stacking configuration of bilayer PTCDA. The in-plane herringbone unit cell is indicated in black, while the unit cell of second layer is depicted in green (α phase: translation along the $\vec{b_1}$ direction) or blue (β phase: translation along the $\vec{b_2}$ direction). b) STM topography image measured across the boundary between first and second molecular layers. From the lateral shift between their respective unit cells, the bilayer PTCDA molecules adopt the α polymorph. c) Height profile along the colored line drawn in (b). Tunneling parameters: b) $V_s = -2.1$ V; $I_t = 50$ pA; 20×20 nm^2.

Declaration of Competing Interest

The authors declare that they have no known competing financial interests or personal relationships that could have appeared to influence the work reported in this paper.

Data availability

Data will be made available on request.

Acknowledgement

The authors dedicate this work in memory of Prof. José María Gómez Rodríguez, personal friend, mentor and colleague. Financial support from the Spanish Ministerio de Economía y Competitividad (MINECO) and Fondo Europeo de Desarrollo Regional (FEDER) under grant No. MAT2016-77852-C2-2-R, as well as, from the Spanish Ministerio de Ciencia e Innovación (MICINN) through the "María de Maetzu" program for units of excellence in R&D (grant No. CEX2018-000805-M) is gratefully acknowledged. A. J. M.-G. acknowledges funding by the Spanish Ministerio de Ciencia e Innovación (MICINN) through Project No. PID2020-116619GA-C22, as well as, from the Comunidad de Madrid and the Universidad Autónoma de Madrid under project SI3/PJI/2021-00500.

References

[1] D. Jariwala, T.J. Marks, M.C. Hersam, Mixed-dimensional Van Der Waals heterostructures, Nat. Mater. 16 (2017) 170–181, https://doi.org/10.1038/nmat4703.
[2] A. Kumar, K. Banerjee, P. Liljeroth, Molecular assembly on two-dimensional materials, Nanotechnology 28 (2017), 082001, https://doi.org/10.1088/1361-6528/aa564f.
[3] M. Gobbi, E. Orgiu, P. Samori, When 2D materials meet molecules: opportunities and challenges of hybrid organic/inorganic Van Der Waals heterostructures, Adv. Mater. 30 (2018) 1706103, https://doi.org/10.1002/adma.201706103.
[4] D. Jariwala, M.C. Hersam, 2D materials: molecular design and engineering perspectives, Mol. Syst. Des. Eng. 4 (2019) 469–470, https://doi.org/10.1039/c9me90017a.
[5] T.O. Wehling, K.S. Novoselov, S.V. Morozov, E.E. Vdovin, M.I. Katsnelson, A. K. Geim, A.I. Lichtenstein, Molecular doping of graphene, Nano Lett. 8 (2008) 173–177, https://doi.org/10.1021/nL072364w.
[6] A.J. Martinez-Galera, N. Nicoara, J.I. Martinez, Y.J. Dappe, J. Ortega, J.M. Gomez-Rodriguez, Imaging molecular orbitals of PTCDA on graphene on Pt(111): electronic structure by STM and first-principles calculations, J. Phys. Chem. C 118 (2014) 12782–12788, https://doi.org/10.1021/jp500768y.
[7] Q.H. Wang, M.C. Hersam, Room-temperature molecular-resolution characterization of self-assembled organic monolayers on epitaxial graphene, Nat. Chem. 1 (2009) 206–211, https://doi.org/10.1038/nchem.212.
[8] J. Wintterlin, M.L. Bocquet, Graphene on metal surfaces, Surf. Sci. 603 (2009) 1841–1852, https://doi.org/10.1016/j.susc.2008.08.037.
[9] M. Batzill, The surface science of graphene: metal interfaces, CVD synthesis, nanoribbons, chemical modifications, and defects, Surf. Sci. Rep. 67 (2012) 83–115, https://doi.org/10.1016/j.surfrep.2011.12.001.
[10] A.J. Martinez-Galera, J.M. Gomez-Rodriguez, Influence of metal support in-plane symmetry on the corrugation of hexagonal boron nitride and graphene

monolayers, Nano Res. 11 (2018) 4643–4653, https://doi.org/10.1007/s12274-018-2045-5.
[11] W. Auwarter, Hexagonal boron nitride monolayers on metal supports: versatile templates for atoms, molecules and nanostructures, Surf. Sci. Rep. 74 (2019) 1–95, https://doi.org/10.1016/j.surfrep.2018.10.001.
[12] K.S. Kim, Y. Zhao, H. Jang, S.Y. Lee, J.M. Kim, K.S. Kim, J.-H. Ahn, P. Kim, J.-Y. Choi, B.H. Hong, Large-scale pattern growth of graphene films for stretchable transparent electrodes, Nature 457 (2009) 706–710, https://doi.org/10.1038/nature07719.
[13] S. Bae, H. Kim, Y. Lee, X.F. Xu, J.S. Park, Y. Zheng, J. Balakrishnan, T. Lei, H. R. Kim, Y.I. Song, Y.J. Kim, K.S. Kim, B. Ozyilmaz, J.H. Ahn, B.H. Hong, S. Iijima, Roll-to-roll production of 30-inch graphene films for transparent electrodes, Nat. Nanotechnol. 5 (2010) 574–578, https://doi.org/10.1038/nnano.2010.132.
[14] T.H. Lee, K. Kim, G. Kim, H.J. Park, D. Scullion, L. Shaw, M.G. Kim, X.D. Gu, W. G. Bae, E.J.G. Santos, Z. Lee, H.S. Shin, Y. Nishi, Z. Bao, Chemical vapor-deposited hexagonal boron nitride as a scalable template for high-performance organic field-effect transistors, Chem. Mat. 29 (2017) 2341–2347, https://doi.org/10.1021/acs.chemmater.6b05517.
[15] C.H. Kim, I. Kymissis, Graphene-organic hybrid electronics, J. Mater. Chem. C 5 (2017) 4598–4613, https://doi.org/10.1039/c7tc00664k.
[16] J. Cho, J. Smerdon, L. Gao, O. Suezer, J.R. Guest, N.P. Guisinger, Structural and electronic decoupling of C_{60} from epitaxial graphene on SiC, Nano Lett. 12 (2012) 3018–3024, https://doi.org/10.1021/nl3008049.
[17] H.G. Zhang, J.T. Sun, T. Low, L.Z. Zhang, Y. Pan, Q. Liu, J.H. Mao, H.T. Zhou, H. M. Guo, S.X. Du, F. Guinea, H.J. Gao, Assembly of iron phthalocyanine and pentacene molecules on a graphene monolayer grown on Ru(0001), Phys. Rev. B 84 (2011), 245436, https://doi.org/10.1103/PhysRevB.84.245436.
[18] J. Lu, P.S.E. Yeo, Y. Zheng, Z.Y. Yang, Q.L. Bao, C.K. Gan, K.P. Loh, Using the graphene Moire pattern for the trapping of C_{60} and homoepitaxy of graphene, ACS Nano 6 (2012) 944–950, https://doi.org/10.1021/nn204536e.
[19] M. Iannuzzi, F. Tran, R. Widmer, T. Dienel, K. Radican, Y. Ding, J.R. Hutter, O. Groning, Site-selective adsorption of phthalocyanine on h-BN/Rh(111) nanomesh, Phys. Chem. Chem. Phys. 16 (2014) 12374–12384, https://doi.org/10.1039/c4cp01466a.
[20] D. Maccariello, M. Garnica, M.A. Nino, C. Navio, P. Perna, S. Barja, A.L.V. de Parga, R. Miranda, Spatially resolved, site-dependent charge transfer and induced magnetic moment in Tcnq adsorbed on graphene, Chem. Mat. 26 (2014) 2883–2890, https://doi.org/10.1021/cm5005467.
[21] J.H. Mao, H.G. Zhang, Y.H. Jiang, Y. Pan, M. Gao, W.D. Xiao, H.J. Gao, Tunability of supramolecular Kagome lattices of magnetic phthalocyanines using graphene-based Moire patterns as templates, J. Am. Chem. Soc. 131 (2009) 14136–14137, https://doi.org/10.1021/ja904907z.
[22] H.T. Zhou, J.H. Mao, G. Li, Y.L. Wang, X.L. Feng, S.X. Du, K. Muellen, H.J. Gao, Direct imaging of intrinsic molecular orbitals using two-dimensional, epitaxially-grown, nanostructured graphene for study of single molecule and interactions, Appl. Phys. Lett. 99 (2011), 153101, https://doi.org/10.1063/1.3646406.
[23] M. Roos, B. Uhl, D. Kunzel, H.E. Hoster, A. Gross, R.J. Behm, Intermolecular Vs molecule-substrate interactions: a combined Stm and theoretical study of supramolecular phases on graphene/Ru(0001), Beilstein J. Nanotechnol. 2 (2011) 365–373, https://doi.org/10.3762/bjnano.2.42.
[24] R. Forker, T. Dienel, A. Krause, M. Gruenewald, M. Meissner, T. Kirchhuebel, O. Groning, T. Fritz, Optical transition energies of isolated molecular monomers and weakly interacting two-dimensional aggregates, Phys. Rev. B 93 (2016), 165426, https://doi.org/10.1103/PhysRevB.93.165426.
[25] F. Schulz, R. Drost, S.K. Hamalainen, P. Liljeroth, Templated self-assembly and local doping of molecules on epitaxial hexagonal boron nitride, ACS Nano 7 (2013) 11121–11128, https://doi.org/10.1021/nn404840h.
[26] X.S. Li, W.W. Cai, J.H. An, S. Kim, J. Nah, D.X. Yang, R. Piner, A. Velamakanni, I. Jung, E. Tutuc, S.K. Banerjee, L. Colombo, R.S. Ruoff, Large-area synthesis of high-quality and uniform graphene films on copper foils, Science 324 (2009) 1312–1314, https://doi.org/10.1126/science.1171245.
[27] G.W. Yuan, D.J. Lin, Y. Wang, X.L. Huang, W. Chen, X.D. Xie, J.Y. Zong, Q.Q. Yuan, H. Zheng, D. Wang, J. Xu, S.C. Li, Y. Zhang, J. Sun, X.X. Xi, L.B. Gao, Proton-Assisted growth of ultra-flat graphene films, Nature 577 (2020) 204–208, https://doi.org/10.1038/s41586-019-1870-3.
[28] H.I. Rasool, E.B. Song, M. Mecklenburg, B.C. Regan, K.L. Wang, B.H. Weiller, J. K. Gimzewski, Atomic-scale characterization of graphene grown on copper (100) single crystals, J. Am. Chem. Soc. 133 (2011) 12536–12543, https://doi.org/10.1021/ja200245p.
[29] Z.Y. Zou, L.L. Patera, G. Comelli, C. Africh, Honeycomb on square lattices: geometric studies and strain analysis of Moire' structures at a symmetry-mismatched interface, J. Phys. Chem. C 124 (2020) 25308–25315, https://doi.org/10.1021/acs.jpcc.0c07251.
[30] S. Kraus, F. Huttmann, J. Fischer, T. Knispel, K. Bischof, A. Herman, M. Bianchi, R. M. Stan, A.J. Holt, V. Caciuc, S. Tsukamoto, H. Wende, P. Hofmann, N. Atodiresei, T. Michely, Single-crystal graphene on Ir(110), Phys. Rev. B 105 (2022), 165405, https://doi.org/10.1103/PhysRevB.105.165405.
[31] A.J. Martínez-Galera, H. Guo, M.D. Jiménez-Sanchez, E. Garcia Michel, J. M. Gomez-Rodriguez, Dirac cones in graphene grown on a half-filled 4d-band transition metal, Carbon 205 (2023) 294–301, https://doi.org/10.1016/j.carbon.2023.01.004.
[32] F.S. Tautz, Structure and bonding of large aromatic molecules on noble metal surfaces: the example of PTCDA, Prog. Surf. Sci. 82 (2007) 479–520, https://doi.org/10.1016/j.progsurf.2007.09.001.
[33] T. Schmitz-Hubsch, T. Fritz, F. Sellam, R. Staub, K. Leo, Epitaxial growth of 3,4,9,10-perylene-tetracarboxylic-dianhydride on Au(111): a Stm and Rheed study, Phys. Rev. B 55 (1997) 7972–7976, https://doi.org/10.1103/PhysRevB.55.7972.
[34] R. Strohmaier, J. Petersen, B. Gompf, W. Eisenmenger, A systematic STM study of planar aromatic molecules on inorganic substrates - I submolecular image contrast, Surface Sci. 418 (1998) 91–104, https://doi.org/10.1016/s0039-6028(98)00685-2.
[35] I. Chizhov, A. Kahn, G. Scoles, Initial growth of 3,4,9,10-perylenetetracarboxylic-dianhydride (PTCDA) on Au(111): a scanning tunneling microscopy study, J. Cryst. Growth 208 (2000) 449–458, https://doi.org/10.1016/s0022-0248(99)00382-6.
[36] B. Krause, A.C. Durr, K.A. Ritley, F. Schreiber, H. Dosch, D. Smilgies, On the coexistence of different polymorphs in organic epitaxy: alpha and beta phase of PTCDA on Ag(111), Appl. Surf. Sci. 175 (2001) 332–336, https://doi.org/10.1016/s0169-4332(01)00082-4.
[37] M. Toerker, T. Fritz, H. Proehl, F. Sellam, K. Leo, Tunneling spectroscopy study of 3,4,9,10-perylenetetracarboxylic dianhydride on Au(100), Surf. Sci. 491 (2001) 255–264, https://doi.org/10.1016/s0039-6028(01)01418-2.
[38] M. Stohr, M. Gabriel, R. Moller, Analysis of the three-dimensional structure of a small crystallite by scanning tunneling microscopy: multilayer films of 3,4,9,10-perylenetetracarboxylic-dianhydride (PTCDA) on Cu(110), Europhys. Lett. 59 (2002) 423–429, https://doi.org/10.1209/epl/i2002-00212-8.
[39] M. Stohr, M. Gabriel, R. Moller, Investigation of the growth of PTCDA on Cu(110): an Stm study, Surf. Sci. 507 (2002) 330–334, https://doi.org/10.1016/s0039-6028(02)01266-9.
[40] E.V. Tsiper, Z.G. Soos, W. Gao, A. Kahn, Electronic polarization at surfaces and thin films of organic molecular crystals: PTCDA, Chem. Phys. Lett. 360 (2002) 47–52, https://doi.org/10.1016/s0009-2614(02)00774-1.
[41] D. Braun, A. Schirmeisen, H. Fuchs, Molecular growth and sub-molecular resolution of a thin multilayer of PTCDA on Ag(110) observed by scanning tunneling microscopy, Surf. Sci. 575 (2005) 3–11, https://doi.org/10.1016/j.susc.2004.10.032.
[42] N. Nicoara, E. Roman, J.M. Gomez-Rodriguez, J.A. Martin-Gago, J. Mendez, Scanning tunneling and photoemission spectroscopies at the PTCDA/Au(111) interface, Org. Electron. 7 (2006) 287–294, https://doi.org/10.1016/j.orgel.2006.03.010.
[43] W. Chen, H. Li, H. Huang, Y.X. Fu, H.L. Zhang, J. Ma, A.T.S. Wee, Two-dimensional pentacene: 3,4,9,10-perylenetetracarboxylic dianhydride supramolecular chiral networks on Ag(111), J. Am. Chem. Soc. 130 (2008) 12285–12289, https://doi.org/10.1021/ja801577z.
[44] J. Ikonornov, O. Bauer, M. Sokolowski, Highly ordered thin films of perylene-3,4,9,10-tetracarboxylic acid dianhydride (PTCDA) on Ag(100), Surf. Sci. 602 (2008) 2061–2068, https://doi.org/10.1016/j.susc.2008.04.009.
[45] M. Wiessner, D. Hauschild, A. Scholl, F. Reinert, V. Feyer, K. Winkler, B. Kromker, Electronic and geometric structure of the PTCDA/Ag(110) interface probed by angle-resolved photoemission, Phys. Rev. B 86 (2012), 045417, https://doi.org/10.1103/PhysRevB.86.045417.
[46] S. Gartner, B. Fiedler, O. Bauer, A. Marele, M.M. Sokolowski, Lateral ordering of Ptcda on the clean and the oxygen pre-covered Cu(100) surface investigated by scanning tunneling microscopy and low energy electron diffraction, Beilstein J. Org. Chem. 10 (2014) 2055–2064, https://doi.org/10.3762/bjoc.10.213.
[47] N. Nicoara, J. Mendez, J.M. Gomez-Rodriguez, Visualizing the interface state of PTCDA on Au(111) by scanning tunneling microscopy, Nanotechnology 27 (2016), 475707, https://doi.org/10.1088/0957-4484/27/47/475707.
[48] N. Nicoara, O. Paz, J. Mendez, A.M. Baro, J.M. Soler, J.M. Gomez-Rodriguez, Adsorption and electronic properties of PTCDA molecules on Si(111)-(7 X 7): scanning tunneling microscopy and first-principles calculations, Phys. Rev. B 82 (2010), 075402, https://doi.org/10.1103/PhysRevB.82.075402.
[49] T. Suzuki, Y. Yoshimoto, K. Yagyu, H. Tochihara, Adsorption of PTCDA on Si(001)-2x1 surface, J. Chem. Phys. 142 (2015), 101904, https://doi.org/10.1063/1.4906118.
[50] A.J. Martinez-Galera, Z. Wei, N. Nicoara, I. Brihuega, J.M. Gomez-Rodriguez, PTCDA growth on Ge(111)-c(2x8) surfaces: a scanning tunneling microscopy study, Nanotechnology 28 (2017), 095703, https://doi.org/10.1088/1361-6528/aa5783.
[51] C. Ludwig, B. Gompf, W. Glatz, J. Petersen, W. Eisenmenger, M. Mobus, U. Zimmermann, N. Karl, Video-STM, LEED and X-ray diffraction investigations of PTCDA on graphite, Zeitschr. Phys. B-Condens. Matter 86 (1992) 397–404, https://doi.org/10.1007/bf01323733.
[52] A. Hoshino, S. Isoda, H. Kurata, T. Kobayashi, Scanning tunneling microscope contrast of perylene-3,4,9,10-tetracarboxylic-dianhydride on graphite and its application to the study of epitaxy, J. Appl. Phys. 76 (1994) 4113–4120, https://doi.org/10.1063/1.357361.
[53] C. Ludwig, B. Gompf, J. Petersen, R. Strohmaier, W. Eisenmenger, STM Investigations of PTCDA and PTCDI on graphite and MoS_2. A systematic study of epitaxy and STM image contrast, Zeitsch. Phys. B-Condens. Matter 93 (1994) 365–373, https://doi.org/10.1007/bf01312708.
[54] C. Kendrick, A. Kahn, S.R. Forrest, Stm study of the organic semiconductor Ptcda on highly-oriented pyrolytic, Appl. Surf. Sci. 104 (1996) 586–594, https://doi.org/10.1016/s0169-4332(96)00207-3.
[55] Y.J. Zheng, Y.L. Huang, Y.F. Chenp, W.J. Zhao, G. Eda, C.D. Spataru, W.J. Zhang, Y.H. Chang, L.J. Li, D.Z. Chi, S.Y. Quek, A.T.S. Wee, Heterointerface screening effects between organic monolayers and monolayer transition metal dichalcogenides, ACS Nano 10 (2016) 2476–2484, https://doi.org/10.1021/acsnano.5b07314.

[56] J. Kroger, H. Jensen, T. Jurgens, T. von Hofe, J. Kuntze, R. Berndt, Adsorption geometry of PTCDA on 2H-$NbSe_2$, Appl. Phys. A-Mater. Sci. Process. 81 (2005) 1285–1289, https://doi.org/10.1007/s00339-004-3039-6.
[57] H. Huang, S. Chen, X.Y. Gao, W. Chen, A.T.S. Wee, Structural and electronic properties of PTCDA thin films on epitaxial graphene, ACS Nano 3 (2009) 3431–3436, https://doi.org/10.1021/nn9008615.
[58] J.M.P. Alaboson, Q.H. Wang, J.D. Emery, A.L. Lipson, M.J. Bedzyk, J.W. Elam, M. J. Pellin, M.C. Hersam, Seeding atomic layer deposition of high-K dielectrics on epitaxial graphene with organic self-assembled monolayers, ACS Nano 5 (2011) 5223–5232, https://doi.org/10.1021/nn201414d.
[59] Q.H. Wang, M.C. Hersam, Nanofabrication of heteromolecular organic nanostructures on epitaxial graphene via room temperature feedback-controlled lithography, Nano Lett. 11 (2011) 589–593, https://doi.org/10.1021/nl103590J.
[60] M. Meissner, M. Gruenewald, F. Sojka, C. Udhardt, R. Forker, T. Fritz, Highly ordered growth of PTCDA on epitaxial bilayer graphene, Surf. Sci. 606 (2012) 1709–1715, https://doi.org/10.1016/j.susc.2012.07.016.
[61] A.J. Martinez-Galera, J.M. Gomez-Rodriguez, Structural and electronic properties of 3,4,9,10-perylene tetracarboxylic dianhydride on h-BN/Rh(110), J. Phys. Chem. C 123 (2019) 1866–1873, https://doi.org/10.1021/acs.jpcc.8b10810.
[62] O. Custance, J.M. Gomez-Rodriguez, A.M. Baro, L. Jure, P. Mallet, J.Y. Veuillen, Low temperature phases of Pb/Si(111), Surf. Sci. 482 (2001) 1399–1405, https://doi.org/10.1016/s0039-6028(01)00774-9.
[63] I. Horcas, R. Fernandez, J.M. Gomez-Rodriguez, J. Colchero, J. Gomez-Herrero, A. M. Baro, WSXM: a software for scanning probe microscopy and a tool for nanotechnology, Rev. Sci. Instrum. 78 (2007), 013705, https://doi.org/10.1063/1.2432410.
[64] P. Lauffer, K.V. Emtsev, R. Graupner, T. Seyller, L. Ley, Molecular and electronic structure of PTCDA on bilayer graphene on SiC(0001) studied with scanning tunneling microscopy, Phys. Status Solidi B-Basic Solid State Phys. 245 (2008) 2064–2067, https://doi.org/10.1002/pssb.200879615.
[65] J.B. Gustafsson, H.M. Zhang, L.S.O. Johansson, STM studies of thin Ptcda films on Ag/Si(111)-Root 3 x Root 3, Phys. Rev. B 75 (2007), 155414, https://doi.org/10.1103/PhysRevB.75.155414.
[66] M. Mobus, N. Karl, T. Kobayashi, Structure of perylene-tetracarboxylic-dianhydride thin films on alkali halide crystal substrates, J. Cryst. Growth 116 (1992) 495–504, https://doi.org/10.1016/0022-0248(92)90658-6.
[67] S.R. Forrest, P.E. Burrows, E.I. Haskal, F.F. So, Ultrahigh-vacuum quasiepitaxial growth of model Van Der Waals thin films, Ii. Experiment, Phys. Rev. B 49 (1994) 11309–11321, https://doi.org/10.1103/PhysRevB.49.11309.
[68] T. Ogawa, K. Kuwamoto, S. Isoda, T. Kobayashi, N. Karl, 3,4,9,10-Perylenetetracarboxylic dianhydride (PTCDA) by electron crystallography, Acta Crystallogr. Sec. B-Struct. Sci. 55 (1999) 123–130, https://doi.org/10.1107/s0108768198009872.
[69] A. Hauschild, K. Karki, B.C.C. Cowie, M. Rohlfing, F.S. Tautz, M. Sokolowski, Molecular Distortions and chemical bonding of a large Pi-conjugated molecule on a metal surface, Phys. Rev. Lett. 94 (2005), 036106, https://doi.org/10.1103/PhysRevLett.94.036106.
[70] L. Yan, Y.B. Zheng, F. Zhao, S.J. Li, X.F. Gao, B.Q. Xu, P.S. Weiss, Y.L. Zhao, Chemistry and physics of a single atomic layer: strategies and challenges for functionalization of graphene and graphene-based materials, Chem. Soc. Rev. 41 (2012) 97–114, https://doi.org/10.1039/c1cs15193b.